

# CRS-BASED SEISMIC IMAGING IN COMPLEX MARINE GEOLOGY

H. Lima, L. Leite, B. Heilmann, and J. Mann

email: hamiltonlim@gmail.com

keywords: CRS Stack, Pre-stack data enhancement, Residual static correction, Migration

## ABSTRACT

*This paper presents results of a consistent workflow for processing and imaging applied to marine seismic data. The data set was collected in the Southern Atlantic offshore Brazil. Searching for techniques to increase the data resolution, fundamental steps of signal processing together with imaging methods based on the data-driven CRS technology, such as CRS-stack based residual static correction and pre-stack data enhancement, were applied and proved to be successful. The final aim of the data processing and imaging sequence was to obtain sections ready to be submitted to geological interpretation. The latter was conducted on the final stacked and CRS time migrated sections. The obtained image panels allow for interpreting discontinuities, thinning, faults, anticlines, plays of horsts and grabens. Some selected parts of the line needed detail processing to make structures more evident that where partly hidden by the strong free surface multiples and diffractions.*

## INTRODUCTION

Recently, Gomes et al. (2007), Heilmann et al. (2007) and Leite et al. (2008) have presented different case studies where CRS-stack-based imaging workflows have been applied to land datasets in order to obtain a better structural image of structures relevant for oil exploration. The present work represents an extension of these efforts to marine data. Main steps of CRS-stack-based seismic imaging were carried out with results that clearly showed improvement on the continuity of reflection events, enhancement in the signal-to-noise ratio, and enhancement of free surface multiples. Previous to the CRS processing, several tasks were performed beginning with the geometry setup, muting of bad shot and receiver gathers,  $f$  filtering,  $f-k$  filtering, deconvolution, field static correction, and spherical divergence correction. The workflow of the present work is summarized in Figure 1, where the major steps follow Heilmann (2007).

Complex geological environments often pose severe difficulties for accurate imaging in time and depth domains, and even more if combined with complicated near surface conditions. Under such circumstances, where simple model assumptions may fail, it is of particular importance to extract as much information as possible directly from the measured data. The Common Reflection Surface (CRS) stack, described by Müller et al. (1998) and Mann (2002), among others, has become a powerful data-driven method for improving the zero-offset (ZO) simulation of seismic data. Topography can be directly considered during the stack process which was irrelevant for the presented marine case. In 2D processing, for every ZO sample three kinematic wavefield attributes are obtained as useful by-products of the stacking process (Hubral, 1999). These attributes have been applied to improve the stack itself, and to support subsequent processing as described in Duvencek (2004), Gamboa (2003), and Koglin (2005), among others. Using the CRS attributes for the transformations between time and depth domains, an advanced data-processing workflow can be established, covering a broad range of seismic reflection imaging issues in a consistent manner.



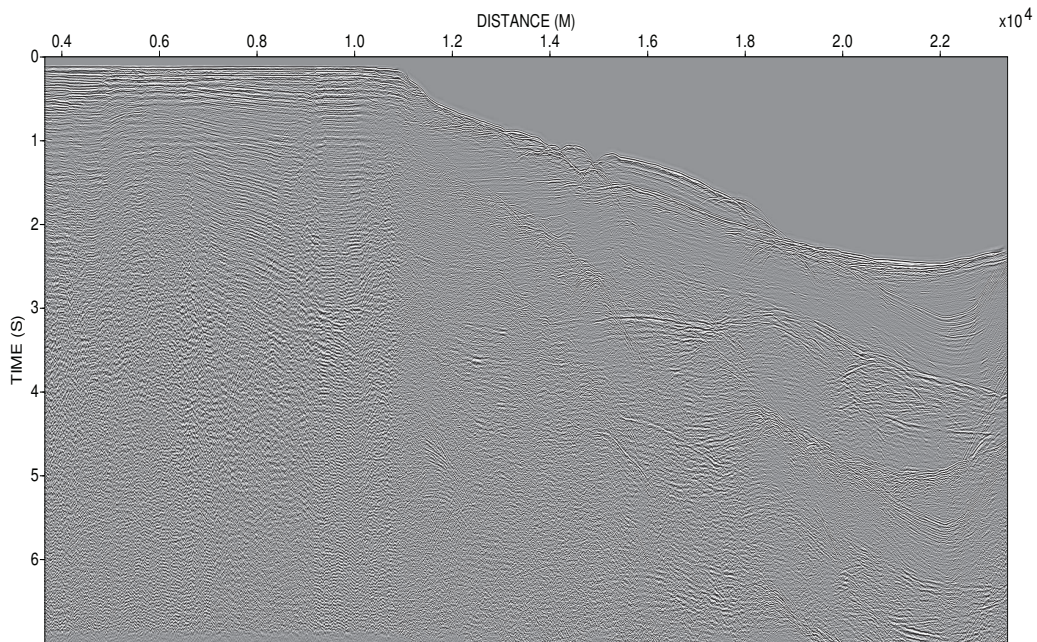


**Figure 3:** Minimum offset section after pre-processing with automatic gain control applied for display.

have reactivated local features that were developed in the rift stage. The stratigraphic scenario is divided into depositional sequences that reflect the geological evolution of the area.

### PRE-PROCESSING

One marine line was selected for presentation, and it has the following general survey information: date of acquisition 1985; direction SE-NW; length 40 km; 1578 shot points; time sampling interval 4 ms; 25 m shot point and receiver station spacing; array guns placed at 8 m depth. The array distributions are from left to right left-unilateral 0-120.

The pre-processing steps were performed with the free seismic processing package CWP/SU of the Colorado School of Mines (Cohen and Stockwell, 2005). The SU data format can easily be created from the original SEG-Y files and directly be used as input for the WIT/CRS codes. Pre-processing consisted of 3 main parts: (1) geometry setting; (2) muting of bad traces; and (3)  $f$  and  $f-k$  filtering. The workflow was organized as an annotated sequence of targets in a `Makefile` with the aim to keep detailed reference information to ensure the reproducibility of the results to emphasize the dependence of the processing on several steps with various parameters. Conventional imaging was applied as well at this stage involving the application of the following techniques: (4) velocity analysis; (5) NMO stacking; (6) migration.

Based on shot and receiver gathers, the original data was analyzed in order to locate noisy shot and receiver sections and to look for dead or corrupted traces. Finally, all strongly corrupted traces were muted. A trapezoidal band-pass filter was applied with corner frequencies of 8-10-70-80 Hz. Furthermore, a  $f-k$  filter was used to suppress unwanted events such as water surface waves and critically refracted waves. The decision for adopting filter parameters was based on the visual analysis of the trace gathers, their spectra, and preliminary stack results that reinforced the importance of the pre-processing. Even though the data is marine, residual static corrections, described by Koglin (2005) was also applied on the basis of geostatistics and communication theory to obtain a better event correlation in the presence of vertical misplacement and source and receiver delays. The Wiener-Hopf predictive error filtering and spiking deconvolution was applied to the data to suppress ocean bottom multiples and to increase the temporal resolution. To show

the results of the pre-processing stage, Figure 3 displays a minimum offset section for reference.

### STACK OPERATOR

As resumed in Bernabini et al. (1987), numerous functionals have been proposed to evaluate quantitatively the fit between measured data and a model function, e. g., parametrized by a stacking velocity value aiming at describing the hyperbolic reflection response of a planar reflector on a given CMP gather. The most common functionals measure the likeness of the corrected gather's amplitude ( $\bar{u}$ ) based on correlation of traces, and choices of normalization. The normalized 2D ( $h, x$ ) measure semblance  $S(t_0; \underline{m})$  is composed by averages, and it is given by

$$S(t_0; \underline{m}) = \frac{\frac{1}{N_t} \sum_{t=t_0-\delta t}^{t=t_0+\delta t} \frac{1}{N_x} \sum_{x=x_F}^{x=x_L} \left[ \frac{1}{N_h} \sum_{h=h_F}^{h=h_L} \bar{u}(h, x; t_0) \right]^2}{\frac{1}{N_t} \sum_{t=t_0-\delta t}^{t=t_0+\delta t} \frac{1}{N_x} \sum_{x=x_F}^{x=x_L} \frac{1}{N_h} \sum_{h=h_F}^{h=h_L} \bar{u}^2(h, x; t_0)}, \quad (\text{where } 0 \leq S \leq 1); \quad (1)$$

for a set of parameters  $\underline{m}$ , from a first half-offset  $h = h_F$  to a last half-offset  $h = h_L$  offset with  $N_h$  points, and for a midpoint  $x$  ranging from  $x_F$  to  $x_L$  with  $N_x$  points, and in a time window specified by some  $\delta t$  around  $t_0$ .  $S(t_0; \underline{m})$  takes values in the interval (0,1) regardless of the absolute signal amplitude, and it quantifies the uniformity of the signal polarity across the NMO corrected gather amplitude  $\bar{u}(t_0; \underline{m})$ . In the NMO stack, the function  $S(t_0; \underline{m})$  can also be interpreted as the function to be optimized, from where optimum a value of stack velocity  $\underline{m} = v$  results.

Conventional velocity analysis is performed on common-midpoint (CMP) gathers by approximating the two-way traveltimes  $t(x; t_0, v)$  of primary reflection arrivals from an interface by a second order hyperbolic model of the type

$$t^2(h; t_0, v) \approx t_0^2 + \frac{4h^2}{v^2}, \quad (2)$$

where  $h$  stands for the half source-receiver offset,  $t_0$  for the normal two-way traveltimes at  $h = 0$ , and  $v$  denotes the stacking velocity. The above law is exact for a single horizontal reflector with homogeneous overburden. For the next level of complexity of the model, one can consider an ideal medium composed of multiple homogeneous, isotropic, layers with horizontal interfaces and small apertures. The above law is still constitutes a reasonably accurate approximation, as described by Ursin (1982).

For NMO correction, the criterion for expressing in quantitative form the degree of fitting between the model described by a stacking velocity value and the data usually involves a coherence measure. A typical algorithm for velocity analysis in the ( $h, t$ ) domain calculates at each point  $t_0$  the velocity spectrum which consists of a coherence value for every stacking velocity  $v$  value within the search range. In practice, often a simple 1D approximation is used to calculate the interval velocities of the medium from the previously determined stacking velocity distribution: the stacking velocity  $v$  is assumed to approximate the root-mean-square (RMS) velocity  $v_{\text{RMS}}$  as described by Al-Chalabi (1992). Turning to a more realistic subsurface, the underground geology can be described by an inhomogeneous velocity distribution that can be smooth or with discontinuities separated by curved interfaces. Under such more general conditions, limitations of the above NMO correction might emerge. The CRS stack concept takes a more complex reflector geometry explicitly into account, which makes it necessary to extent the velocity analysis from the 2D time-offset space to the 3D time-offset-midpoint domain.

The CRS stacking method does not explicitly depend on a macro-velocity model in the ( $x, t$ ) domain. It employs an automatic data-driven parameter search based on semblance analysis (1) in the prestack data and can thus be seen as an optimization problem where the objective function is the semblance value related to a certain parameter combination. The CRS stack operator can be derived from paraxial ray theory or homeomorphic imaging concepts and constitutes a second-order traveltimes formulation for 2D and 3D inhomogeneous models with arbitrarily curved interfaces. This traveltimes operator is parametrized using two notional eigenwave experiments generating the so-called normal-incidence-point (NIP) wave and the normal (N) wave. The NIP wave is associated with an exploding diffractor (or point source) at the normal-incidence point NIP of the zero-offset ray. This produces the NIP wave which reaches the surface at  $x_0$

with the radius  $R_{\text{NIP}}$ . The N-wave is associated with an exploding reflector around the NIP location and generates the normal wave which reaches the surface at  $x_0$  with of radius  $R_N$ .

In the context of paraxial ray theory, we consider a central ray with normal incidence on the reflector at the NIP. Furthermore, only primary events taken into account. The central ray satisfies Snell's law across the interfaces, and the wavefront curvatures of the NIP and N waves change according to the refraction and transmission laws of curvature, as described in Hubral and Krey (1980). Following Schleicher et al. (2007), the hyperbolic approximation for the two-way traveltimes of primary reflections from a curved interface on a flat observation surface is given by

$$t_{\text{hyp}}^2(x_m, h) = \left[ t_0 + \frac{2 \sin \beta_0 (x_m - x_0)}{v_0} \right]^2 + \frac{2t_0 \cos^2 \beta_0}{v_0} \left[ \frac{(x_m - x_0)^2}{R_N} + \frac{h^2}{R_{\text{NIP}}} \right]. \quad (3)$$

$P_0(x_0, t_0)$  is the reference point of stack, and it is assumed that the velocity  $v_0$  is known and related to the upper layer and around the observation point  $x_0$ . The independent variables  $x_m$  and  $h$  are the shot and receiver midpoint coordinate and the half-offset, respectively. The parameter  $\beta_0$  corresponds to the vertical emergence angle of the wavefront at the observation point  $x_0$ . The quantities  $\beta_0$ ,  $R_{\text{NIP}}$ , and  $R_N$  are related to the central ray in the paraxial ray theory.

For the practical work, the data headers contain the CDP numbers, the source coordinates  $x_S$ , and the receiver coordinates  $x_G$ . Their relationship to the  $x_m$  and  $h$  coordinates and are given by  $x_m = (x_G + x_S)/2$  and  $h = (x_G - x_S)/2$ . The semblance analysis is performed along the spatial stacking operator (3) spanned by the coordinates  $h$  and  $x_m$  according to Equation (1). The vector  $\underline{m}$  takes the values  $\underline{m} = (R_{\text{NIP}}, R_N, \beta_0; v_0)$ , where the parameters  $R_{\text{NIP}}$ ,  $R_N$ , and  $\beta_0$  (with  $v_0$  fixed) are searched for as an optimization problem with the semblance (1) as object function, and the CRS operator (3) as the forward model. The parameter search is classified as a nonlinear ill-posed problem; therefore the strategy may need a starting point in the parameter space and derivatives, or a controlled random search without derivatives. Müller et al. (1998) and Mann (2001a) describe strategies for the parameter search, basically performed in four steps.

Mann (2001b) described the problem related to conflicting dips in the stack sections, analyzed the dependence of  $v_{\text{NMO}}$  on  $\beta_0$ , and proposed a solution to this problem by detecting multiple values  $\beta_0$  for each contributing event by adapting the original search strategy of Müller et al. (1998). Soleimani et al. (2009) addresses the conflicting dip problem by proposing a strategy that considers a multitude of different values of  $\beta_0$  for each ZO sample, with the forward model (3) under the condition  $R_N = R_{\text{NIP}}$ , to improve the continuity of reflection events and diffraction events, in a process named common-diffraction-surface stack.

## CRS MIGRATION

A Kirchhoff-type time migration scheme is integrated in the CRS stack algorithm. This application proposed by Mann (2002) considers that the CRS attributes allow to approximate the (hypothetical) diffraction event associated with reflection event in the data, and, thus, a Kirchhoff migration operator. The apex of the ZO diffraction response provides an approximation of the image location for time migration. Due to the symmetry considerations,  $\partial t_{\text{hyp}}(x_m, h = 0)/\partial x_m = 0$  for the ZO plane  $h = 0$ . This yields the apex location

$$x_{\text{apex}} = x_0 - \frac{R_{\text{NIP}} t_0 v_0 \sin \beta_0}{2R_{\text{NIP}} \sin^2 \beta_0 + t_0 v_0 \cos^2 \beta_0}, \quad (4)$$

$$t_{\text{apex}}^2 = \frac{t_0^3 v_0 \cos^2 \beta_0}{2R_{\text{NIP}} \sin^2 \beta_0 + t_0 v_0 \cos^2 \beta_0}. \quad (5)$$

This approximate ZO diffraction response can be parametrized in terms of the apex location  $(x_{\text{apex}}, t_{\text{apex}})$  instead of the ZO location  $(x_0, t_0)$ :

$$t_{\text{hyp}}^2(x) = t_{\text{apex}}^2 + \frac{4(x - x_{\text{apex}})^2}{v_c^2}, \quad \text{with} \quad (6)$$

$$v_c^2 = \frac{2v_0^2 R_{\text{NIP}}}{2R_{\text{NIP}} \sin^2 \beta_0 + t_0 v_0 \cos^2 \beta_0}. \quad (7)$$

A summation along the approximate diffraction response, with its result assigned to its apex, approximates a Kirchhoff time migration. Even more convenient, the already available stack value computed along the CRS operator can be assigned to the apex  $(x_{\text{apex}}, t_{\text{apex}})$ .

### RESIDUAL STATIC CORRECTION

Aiming at increasing resolution, the static residual correction strategy has been applied under the concept of virtual source-receiver vertical and horizontal displacements, and in terms of communication theory looking for better correlation between the ZO trace and its corresponding family's traces under small shifts. Koglin (2005) and Koglin et al. (2006) describe in detail the CRS-based residual static correction as an iterative process similar to the super-trace cross-correlation method as presented by Ronen and Claerbout (1985). In this approach, the cross-correlations are performed within the CRS super gathers consisting of all moveout corrected prestack traces within the spatial stacking aperture, instead of being confined to individual CMP, common-shot or common-receiver gathers. Due to the spatial extent of the employed stacking operator, a super gather contains many neighboring CMP gathers. For each considered super gather centered around a particular ZO location, the moveout correction will, in general, be different. Since each prestack trace is included in many different super gathers, it contributes to more cross-correlations than in methods using only individual gathers. The cross-correlations of the stacked pilot trace and the moveout corrected prestack traces are summed up for each shot and receiver location. This summation is performed for all super gathers contained in the specified target zone. The searched for residual time shifts are then expected to be associated with the locations of the maxima in the cross-correlation stacks, and they are used to correct the prestack traces. The stack result after residual static correction is presented and we observed an improvement in resolution.

### PRESTACK DATA ENHANCEMENT

As a next step aiming at increasing resolution, the concept of prestack data enhancement by interpolating new CDPs based on the CRS stack operator and data driven attributes as described by Baykulov and Gajewski (2007) has been integrated into the processing workflow. The CRS-based interpolation constructs super gathers to prescribed positions  $x_m$ , and results in better lateral resolution whereby the size of projected Fresnel zone is used for the lateral window control. Using the CRS attributes  $\beta_0$  and  $R_{\text{NIP}}$ , the corresponding time obtained from the  $t_0$  is given by

$$t^2(x_m, h) = \left( -\frac{h^2 \cos^2 \beta_0}{v_0 R_{\text{NIP}}} + \sqrt{\left( \frac{h^2 \cos^2 \beta_0}{v_0 R_{\text{NIP}}} \right)^2 + t^2 + \frac{2 \sin \beta_0}{v_0} x_m} \right)^2 + \frac{2 \cos^2 \beta_0}{v_0} \left( -\frac{h^2 \cos^2 \beta_0}{v_0 R_{\text{NIP}}} + \sqrt{\left( \frac{h^2 \cos^2 \beta_0}{v_0 R_{\text{NIP}}} \right)^2 + t^2} \right) \left( \frac{x_m^2}{R_N} + \frac{h^2}{R_{\text{NIP}}} \right). \quad (8)$$

Depending on the quality of the data and on the acquisition geometry, the lateral windows for stacking can be optimized in the directions  $x_m$  and  $h$ . In our examples the sizes were the same as chosen in the CRS stack.

### RESULTS AND DISCUSSIONS

Our main attention in the present work was directed to the following CRS results: (1) optimized stack; (2) migration; and (3) multiple enhancement. The stack serves as the basis for the migration to collapse diffractions, and for the post-stack multiple enhancement to serve for further development and application of techniques for multiple attenuation. For these aims, the results are shown in the following order: (1) coherence; (2)  $R_{\text{NIP}}$ , (3)  $1/R_N$ ; (4) angle; (5) optimized Fresnel stack; (6) interpreted optimized Fresnel stack; (7) optimized time migration; (8) interpreted optimized Fresnel time migration.

The analysis of the results starts with the minimum offset panels depicted in Figure 3 which serve as reference to the stack and migration results. The CRS results are controlled by the distribution of semblance values in the coherence panel, which is used to identify locations with very low coherence

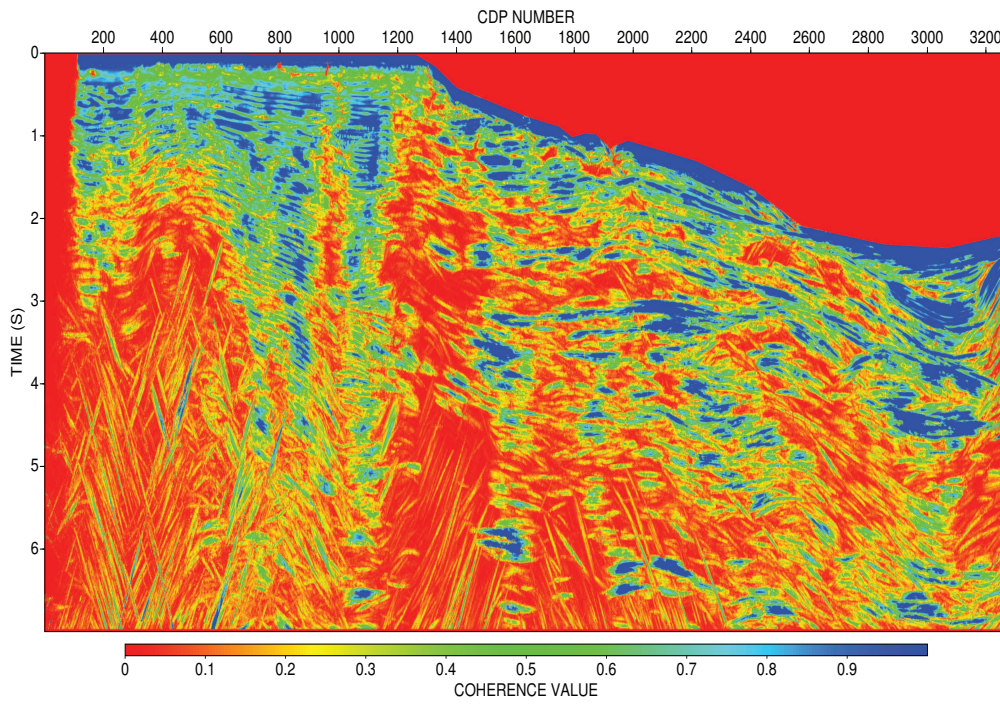


**Figure 4:** Coherence section of CRS super gather stack.

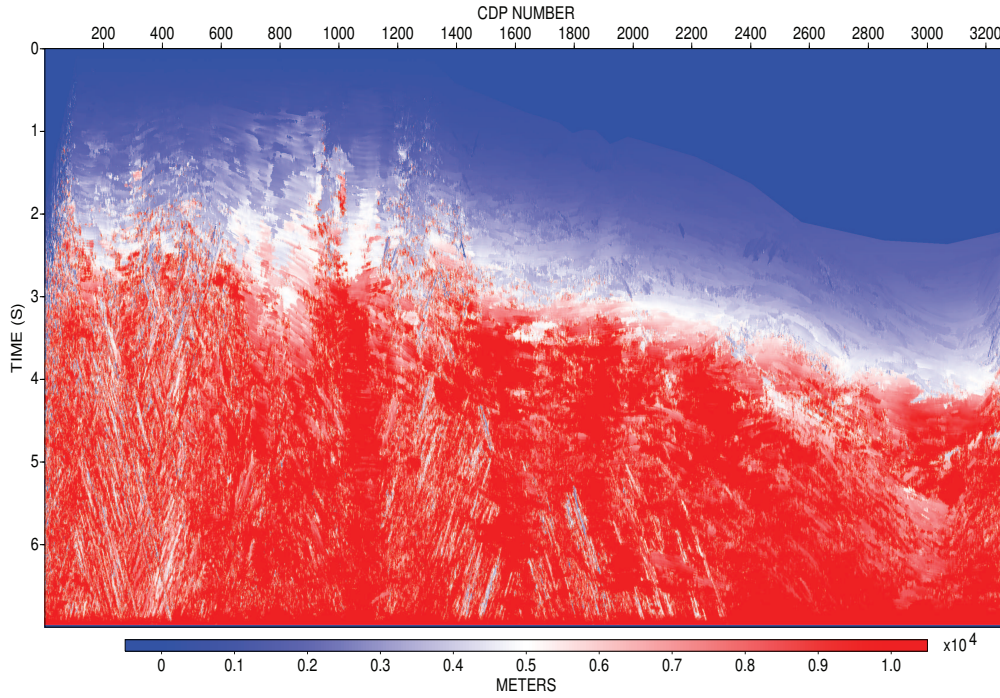


**Figure 5:**  $R_{NIP}$  section of CRS super gather stack.

values, considering that such locations are not expected to be associated with reliable attributes ( $R_{\text{NIP}}$ ,  $R_{\text{N}}$ ,  $\beta_0$ ) to obtain the stacking parameters of the CRS operator.

The panels of the kinematic CRS wavefield attributes  $R_{\text{NIP}}$ ,  $1/R_{\text{N}}$  and  $\beta_0$  are shown in Figures 5, 6 and 7, respectively. Where the latter two panel show structural trends in a similar way as the stack and migration panels, the  $R_{\text{NIP}}$  has more similarity to an (unsmoothed) stacking velocity model.

## CONCLUSIONS

We are here restricted to the geometrical interpretation of geological structures carried out mainly on the basis of migrated sections and stacked sections. The meaning of the interpreted lines in these figures are colored as: (red) horizontal and dipping reflectors; (blue) multiples; (yellow) reflectors as anticline; (green) vertical discontinuities.

The analysis of the stack section in Figure 8, comparing with the Kirchhoff-type time migration section in Figure 10, clearly shows the seafloor followed by the response of basin sediments with several reflectors with similar geological attitude. These events are intersected by free surface multiples and diffraction events. On the other hand, the migration panels do not present the effect of the diffractions by showing the collapsing points.

For the stack, the main panel for interpretation is Figure 8 to result in Figure 9. For the migration, the main panel is Figure 10. To compare the results of the CRS Kirchhoff-type migration with the stack itself, the interpreted colored lines in Figure 9 were superimposed onto Figure 10 to result in Figure 11. From these Figures 9 and 11 one can see only slight shifts between events and drawn lines, what establishes both sections being useful for tracking structures.

For drawing the structures, it is important that the section have the proper scale, axis exaggeration, and size. From screen color display and details of the used figures and zooms, discontinuities, thinning, anticlines, faults, plays of horsts and grabens, and rollovers can be identified. On the other hand, the basement is not easily traced, and the left part of the section needs more attention for structures to be better recognized. Figure 11 shows details of reflector zones related to stratigraphical units. One of the most prominent features is on the left side and can be interpreted as intrusions.

The quality of the marine seismic data is not a decisive limitation in enhancing different parts for the imaging of the selected line. The intention with this conclusion is to geometrically trace structures and to demonstrate the applicability of the CRS stack and and its integrated time migration towards basin reevaluation providing a good basis for geological interpretation and, hopefully, for successful drilling.

The coherence sections served to indicate the fit between the CRS stacking operators and the primary reflection events in the prestack data. We consider that the overall quality of the marine seismic underground image is quite reasonable compared to other high quality seismic images that served as reference for the present processing. Even though, the results obtained by CRS revealed good resolution as measured by signal-to-noise ratio and reflector continuity. We call attention to the fact of the granular appearance of the migration panel, a consequence of the point-to-point mapping inherent to this strategy.

This example serves also to reinforce our perspectives and intentions on research collaboration between different universities, and between university and industry to provide development and human resources for the established seismic technology for oil and gas exploration. The research is part of the continuous cooperation between the Faculty of Geophysics of the Federal University of Pará (Brazil) and Karlsruhe Institute of Technology, Germany.

## ACKNOWLEDGMENTS

The authors would like to thank the Brazilian institutions UFPA (Universidade Federal do Pará), FINEP (Financiadora de Estudos e Projetos), ANP (Agência Nacional do Petróleo) and PETROBRAS (Petróleo Brasileiro S/A) for the research support. The thanks are also extended to CAPES and CNPq for the scholarships of Hamilton M. Lima Jr. The authors would like also to thank the reviewers for the useful comments and suggestions for improving this paper.

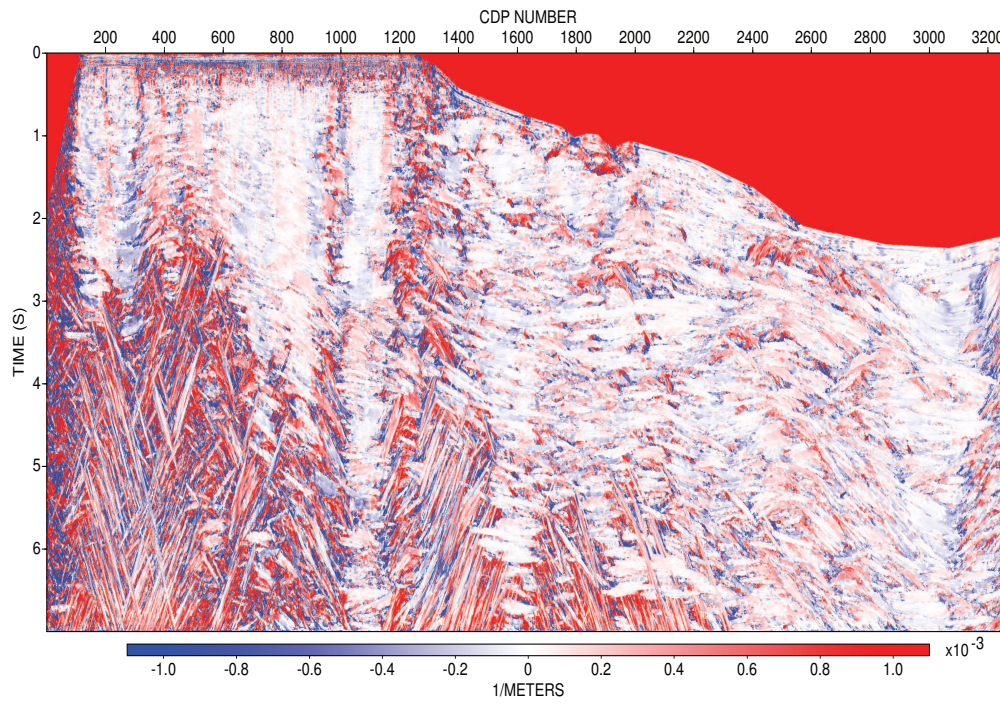


**Figure 6:**  $1/R_N$  curvature section of CRS super gather stack.

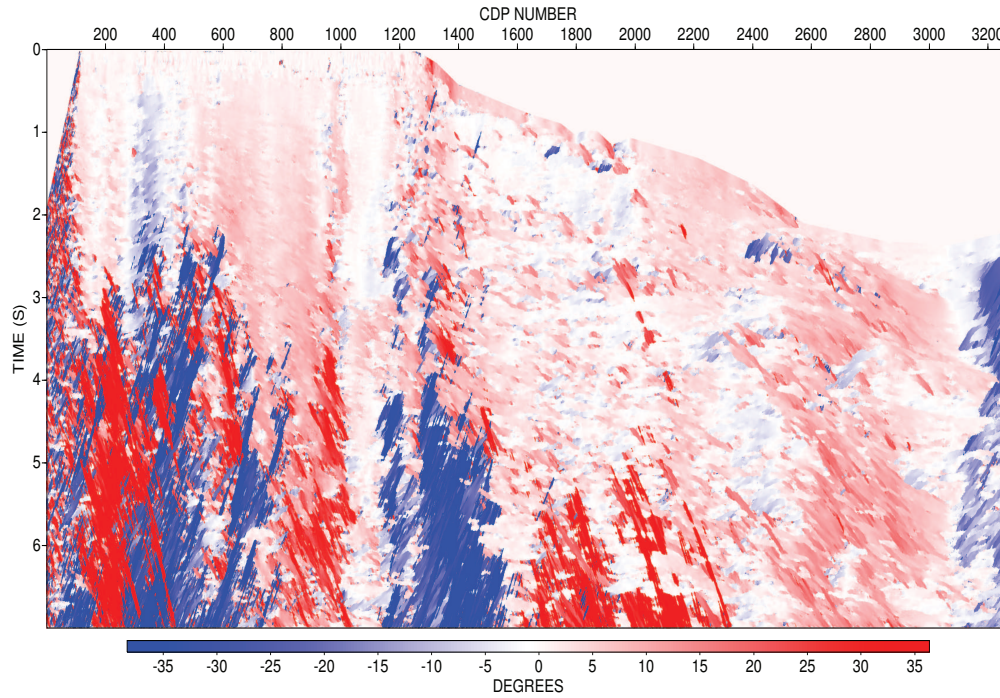


**Figure 7:** Angle  $\beta_0$  section of CRS super gather stack.

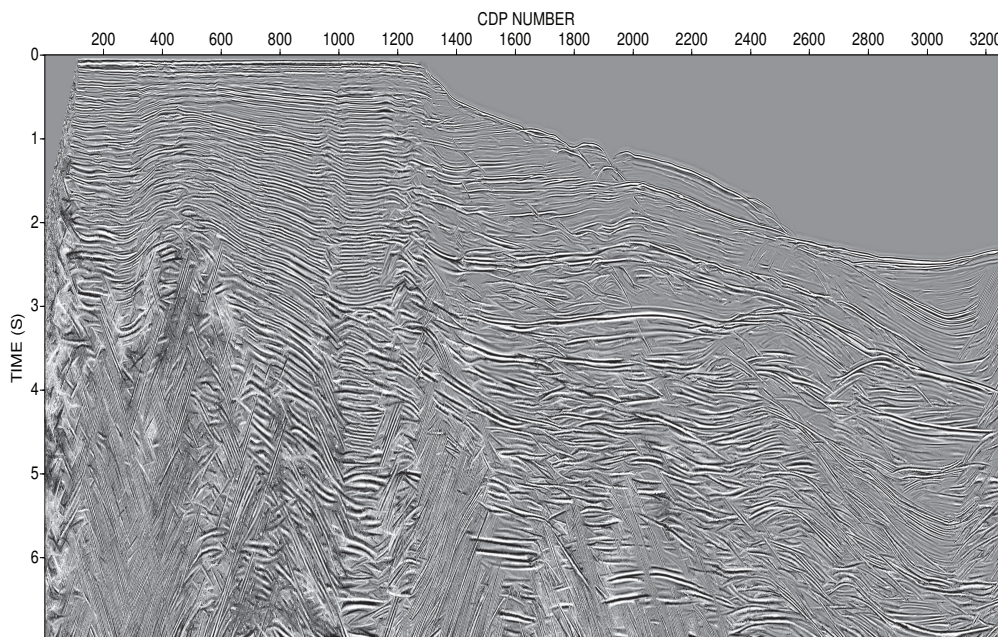


**Figure 8:** Optimized CRS Fresnel super gathers stack.

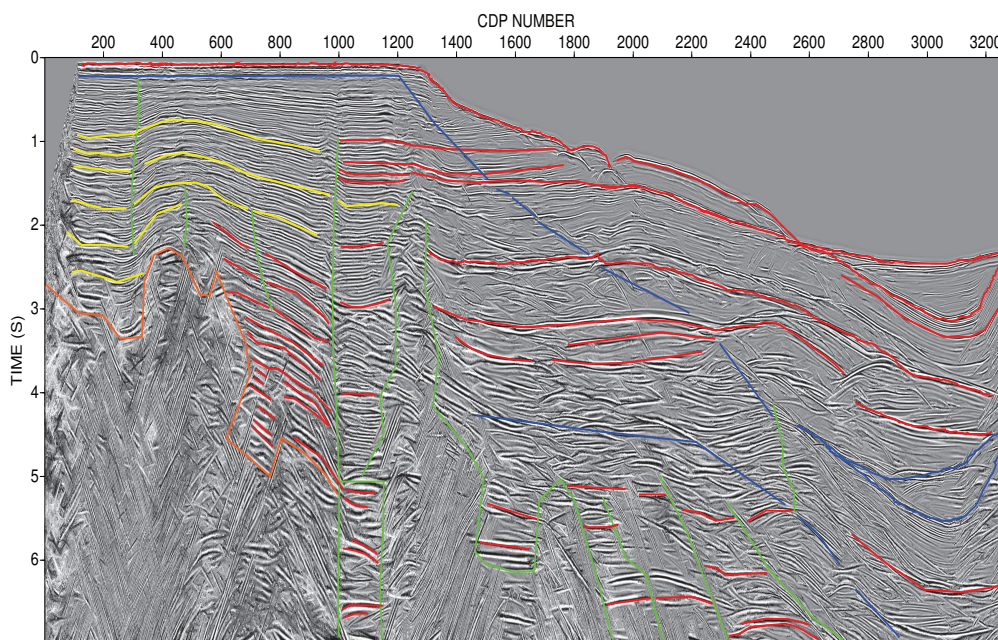


**Figure 9:** Interpreted optimized CRS super gathers stack for geometrical structures.

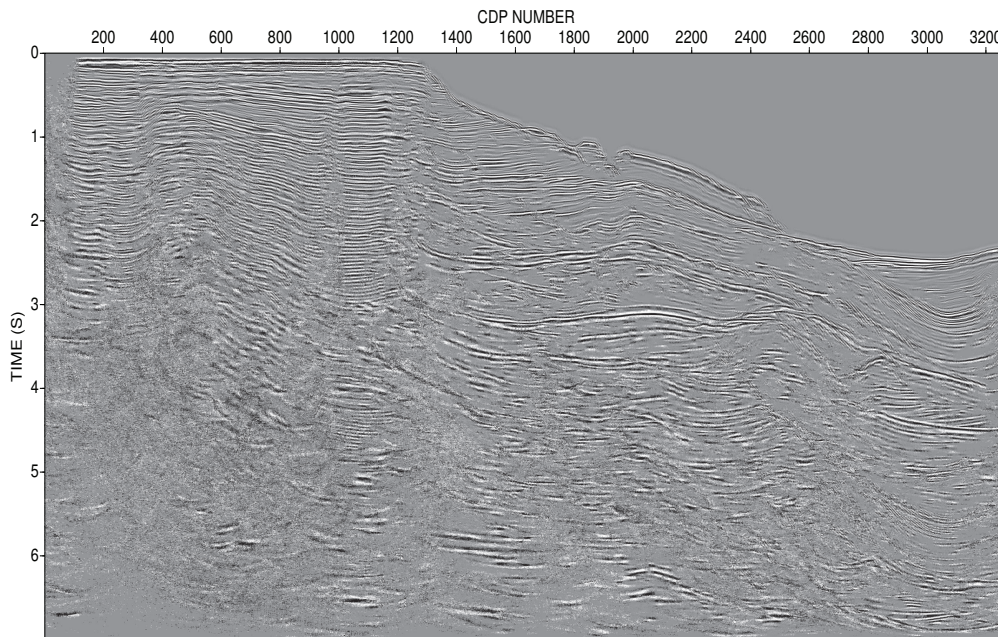


**Figure 10:** CRS Fresnel and super gathers post-time Kirchhoff-type migration section.

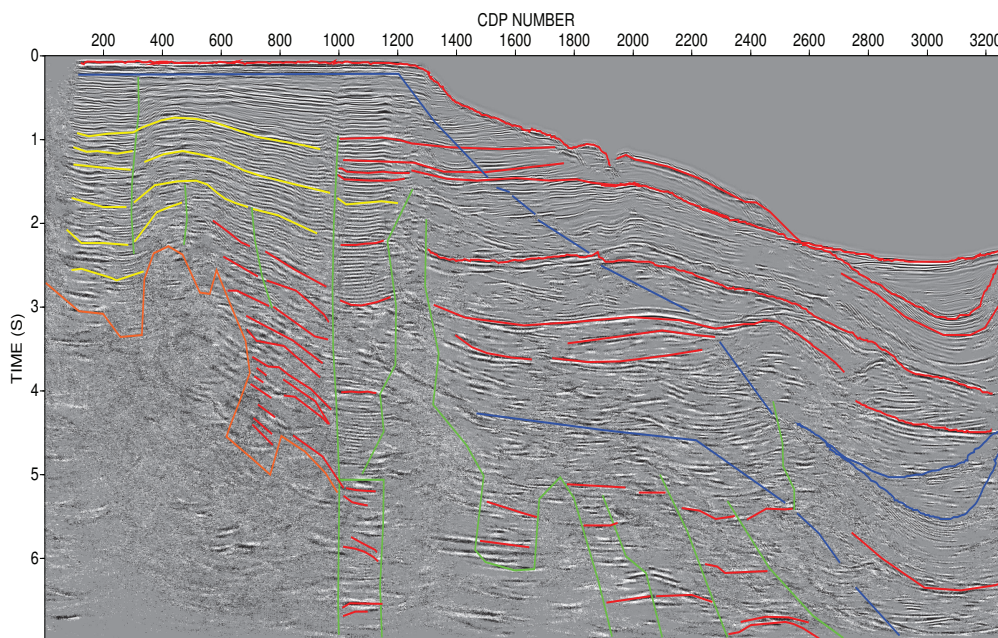


**Figure 11:** Interpreted optimized CRS super gathers post-time Kirchhoff-type migration for geometrical structures. The interpreted colored lines in Figure 9 were transported to the CRS Kirchhoff-type migration of Figure 10.

## REFERENCES

- Al-Chalabi, M. (1992). When 'least-squares' squares least. *Geophys. Prosp.*, 40(03):359–378.
- Baykulov, M. and Gajewski, D. (2007). Prestack seismic data enhancement with CRS parameters. In *Ann. report*, volume 11, pages 50–61. Wave Inversion Technology Consortium.
- Bernabini, M., Carrion, P., Jacovitti, G., Rocca, F., Treitel, S., and Worthington, M. H. (1987). *Deconvolution and inversion*. Blackwell Scientific Publications.
- Cohen, J. K. and Stockwell, J. J. W. (2005). *CWP/SU: Seismic Unix Release 39 – a free package for seismic research and processing*. Center for Wave Phenomena, Colorado School of Mines.
- Duveneck, E. (2004). *Tomographic determination of seismic velocity models with kinematic wavefield attributes*. Logos Verlag, Berlin.
- Gamboa, F. (2003). *Caracterização e Eliminação de Múltiplas pelo Método da Superfície Comum de Reflexão (CRS)*. PhD thesis, UNICAMP, Universidade Estadual de Campinas, São Paulo, Faculdade de Engenharia Mecânica, Instituto de Geociências.
- Gomes, A. B., Leite, L. W. B., Sadala, L., Pestana, R. C., Aldunate, G. C., and Mann, J. (2007). Modeling, stack and imaging. *10th International Congress of the Brazilian Geophysical Society*.
- Heilmann, B. Z. (2007). *CRS-stack-based seismic reflection imaging for land data in time and depth domains*. PhD thesis, Karlsruhe University, Karlsruhe.
- Heilmann, B. Z., Leite, L. W. B., and Gomes, A. B. (2007). Basin reevaluation by CRS. *10th International Congress of the Brazilian Geophysical Society*.
- Hubral, P. (1999). Macro-model independent seismic reflection imaging. *Journal of Applied Geophysics*, 42(3,4).
- Hubral, P. and Krey, T. (1980). *Interval Velocities from Seismic Reflection Time Measurements*. Society of Exploration Geophysicists, Tulsa, OK.
- Koglin, I. (2005). *Estimation of residual static time shifts by means of the CRS-based residual static correction approach*. Logos Verlag, Berlin.
- Koglin, I., Mann, J., and Heilmann, Z. (2006). CRS-stack-based residual static correction. *Geophysical Prospecting*, 54:697–707.
- Leite, L. W. B., Heilmann, B. Z., and Gomes, A. B. (2008). CRS seismic data imaging. *Revista Brasileira de Geofísica*, 25(3):321–336.
- Mann, J. (2001a). *Common-reflection-surface stack*. Geophysical Institute, University of Karlsruhe, Karlsruhe, Germany.
- Mann, J. (2001b). Common-Reflection-Surface stack and conflicting dips. In *Extended abstracts, 63rd Conf. Eur. Assn. Geosci. Eng. Session P077*.
- Mann, J. (2002). *Extensions and applications of the Common-Reflection-Surface Stack method*. Logos Verlag, Berlin.
- Mohriak, W., Szatmart, P., and Anjos, S. M. C. (2008). *Sal*. Editora Beca, Rua Capote Valente, 779 - São Paulo, primeira edição edition.
- Müller, T., Jäger, R., and Höcht, G. (1998). Common Reflection Surface stacking method – imaging with an unknown velocity model. In *Expanded abstracts, 68th Ann. Internat. Mtg.*, pages 1764–1767. Soc. Expl. Geophys.

- Ronen, J. and Claerbout, J. F. (1985). Surface-consistent residual statics estimation by stack-power maximization. *Geophysics*, 50(12):2759–2767.
- Schleicher, J., Tygel, M., and Hubral, P. (2007). *Seismic True-Amplitude Imaging*. Society of Exploration Geophysics.
- Soleimani, M., Piruz, I., Mann, J., and Hubral, P. (2009). Solving the problem of conflicting dips in Common-Reflection-Surface stack. In *Extended Abstracts, 1st Internat. Conf. & Exhib., Shiraz, Iran*. Eur. Assn. Geosci. Eng.
- Ursin, B. (1982). Quadratic wavefront and travelttime approximations in inhomogeneous layered media with curved interfaces. *Geophysics*, 47(7):1012–1021.